ASTFE
American Society
of Thermal and Fluids Engineers

7th Thermal and Fluids Engineering Conference (TFEC)
April–May, 2022
Partially Online Virtual and in Las Vegas Conference

TFEC-2022-40491

# UNDERSTANDING THE INFLUENCE OF PRESSURE DISTURBANCE ON THE TRANSITION OF STRATIFIED TO SLUG FLOW

**Pratik Mahyawansi,[1] Cheng-Xian Lin,[1,*] & Arturo S. Leon[2]**

[1]Dept. of Mechanical and Materials Engg, Florida International University, Miami, Florida, 33174
[2]Dept. of Civil and Environmental Engg, Florida International University, Miami, Florida, 33174

## ABSTRACT

The formation of slug flow in horizontal pipes governs the characteristics of geyser events in storm sewers. In this work, horizontal pipe is decoupled from the vertical pipe, and the newly formed boundary is subjected to sinusoidal disturbance to investigate the response of the gas-liquid interface. The role of pressure disturbance is greatly influenced by the initial pressure and velocity conditions, and the pipe's diameter and length. Using the non-dimensional momentum equation, we identified two significant non-dimensional parameters, coefficient of pressure gradient and coefficient of shear stress rate as a function of the operating conditions and dimension of the system. These parameters directly influence the pressure gradient and viscous effects in the momentum equations and thereby the formation of slugs. This hypothesis is analyzed using 2D numerical simulations in Ansys Fluent for various operating conditions (pressure head 3 times to 50 times pipe diameter) and pipe lengths (10 to 1000 times pipe diameter). Since we are interested in the qualitative analysis of slugs distribution and not the exact shape and slugs' volume fraction details, 2D simulation methodology is adopted. The two non-dimensional parameters justified the numerical results for the dramatic events of slug flow and large wave formations. It is seen that, large values of the coefficient of pressure gradient enhances the possibility of slug formations, whereas the magnitude of the shear stress rate coefficient governs the scale of influence along the length of the pipe. These findings could provide insights on the mitigation of unwanted slug formation encountered in multiphase flow systems.

**KEY WORDS:** Slug flow, Stratified flow, Multiphase flow, Geyser, VOF,

## 1. INTRODUCTION

The gas-liquid interface in a stratified flow tends to break and allow local accumulation of liquid and gas in certain operating conditions. The liquid between two successive gas pockets is called slug that moves at gas speed and the flow regime is called slug flow. This flow type is encountered in various industrial processes such as in oil distillery transport pipes, condenser pipes, and storm sewers. The size of slugs can grow or reduce depending on the local hydro-static pressure. Previous researchers have shown that for a steady flow and in a controlled environment, the slug formation is directly related to the ratio of superficial velocities of gas and liquid [10]. As per Kelvin-Helmholtz instability theory, the mechanism of the transition of stratified to slug flow is due to high gas velocities, which generates enough pressure disturbance on the interface to surpass the stabilizing effect of gravity [14]. An important question after slug formation is the statistical distribution of slugs and their velocities. Also, the aeration or volume fraction of liquid in the slug is an important aspect of such flows as it governs the severity of the damage and vibration in the pipes. It has been shown through visualization techniques that the propensity of aeration is highest for high gas flow rates [17].

*Corresponding Cheng-Xian Lin: lincx@fiu.edu

In a geyser experiment consisting of vertical and horizontal pipes, Leon et al. [12] showed the generation of large slugs in the horizontal pipes due to Taylor-like bubble rising in the vertical pipe followed by water spillage. The spillage at the top of the vertical pipe caused a depressurization in the vertical pipe that induces slug formation in the horizontal pipe.These slugs were propelled to the vertical pipe causing rapid consecutive eruptions of air-water mixtures with heights exceeding 30 m. Also, Chegini and Leon [3] showed this phenomenon numerically, where the pressure in the pipe is found to fluctuate by around 20 percent of the initial pressure with a low frequency of disturbance dominating the physics. The current work is motivated by these results, where we aim to investigate the initiation of slugs due to pressure disturbance and establish the links between the operating conditions and probability of slug formations.

## 2. CURRENT STATE OF ART

Slug flow has been investigated for the past seven decades where early research focused on vertical pipes and the steady movement of slugs have been observed, and correlations were reported to predict the velocity of the large bubbles [5, 8] . However, for horizontal pipes, the concept of slug productions and their movements are quite counter-intuitive, and a plethora of research has been conducted. Additionally, slugs can coalesce or break into smaller slugs and result in non-uniform distribution. Olbrich et al. [16] studied the coherent structure of slug flow using experiments and numerical techniques for pipes with a diameter of 0.0972 m and a length of 9.72 m and reported their length and frequency. The slugs were introduced using sinusoidal variation in the interface at the inlet boundary. The paper also showed an image processing technique to capture interface from the animation data and thereby calculate slugs' statistical characteristics. Also, they showed the velocity of the slugs could be calculated using the correlation of the two successive interface signals. Conte et al. [4] studied the initiation of slugs from the stratified flow, generated by a $3^o$pipe bend. The flow of air and water was independently controlled, and slugs were measured using resistive sensors. The study showed the distribution of slug sizes and frequencies for various flow conditions and reported early slugs formation for high liquid flow rates.

Dukler and Hubbard [6] conducted experiments on the slug flow in a horizontal pipe, and based on the visual observation of the dynamics of the slugs; they proposed model to predict slug length, velocity, and frequency for given flow rates, fluid properties, and pipe geometry. The efficacy of the model is tested against experimental results, and the prediction is very promising for slug frequencies, whereas for slug lengths, the model has a significant error in magnitude albeit capturing the trend. Nydal et al. [15] conducted experiments on horizontal pipes to study slug flows. The study mainly focused on the statistical analysis of both fully developed and developing slugs and slug length distribution was found to be well-fitted by a log-normal distribution. Also, the slug length is found to be insensitive to the flow rates. Greskovich and Shrier [7] investigated slug frequency by considering the volume fraction and Froude number of the mixture. The study reported a chart of slug frequency and test data were compared against the correlation of Hubbard and Dukler [9] and showed for large pipe diameter, the results are quite off from the predictions. Apart from flow conditions, the diameter of pipe also plays an important role in the slug frequencies and length. Larger diameter pipes requires higher liquid superficial velocities to attain slug flow [11]. Taitel and Dukler [18] showed the effect of pipe length on the hydrodynamic slug's characteristics. However, these effects are only seen for the extreme flow conditions (large difference in gas and liquid superficial velocities) for the larger diameter pipes [2].

Previous work mostly focused on ambient pressure conditions and small diameter pipes. The fundamental understanding of the transition from stratified to slug flow at elevated pressure and large pipes is still open for research. In this work, we first analyze the combined-phase X-momentum equation in 2D stratified flow and identify *two key non-dimensional parameters* that influences slug generations. Second, we numerically validate the effect of the identified parameters on a stratified flow excited by harmonic pressure disturbance. In previous works, slugs were generated by controlling the flow rate and maintaining it at a constant value; this limits our understanding to only steady flows. We use the total pressure boundary, which allows the flow to accelerate or decelerate, allowing slugs to initiate naturally.

## 3. MATHEMATICAL FORMULATION AND SOLUTION

In the preliminary analysis, we perform numerical simulations for the transition from stratified to slug flow in a 2D pipe of length 100 m and diameter 1 m due to pressure disturbance at its outlet boundary. It is noted that, the response of the liquid to a pressure disturbance in the stratified flow is a key driving factor in the generation of slugs. The response is highly damped for lower operating pressure, and it is very sensitive at higher operating pressure. Based on these results, we investigate the contribution of the operating conditions in the governing equations. In the following sections, first we discuss the governing equations used to solve the multiphase flow physics. Second, we explore X-momentum equation and derive the coefficients of the gradients that plays key role in the generation of slugs.

### 3.1 Governing Equations

We set up a 2D numerical study in Ansys Fluent-R19 [1] for modelling multiphase flow. In two-phase flow, the continuity equation (Equation-1) is solved for one phase with volume fraction, generally compressible phase for better solver stability.

$$\frac{\partial(\alpha_2\rho_2)}{\partial t} + \nabla.(\alpha_2\rho_2\vec{V_2}) = 0 \tag{1}$$

Here, $\alpha_2$ is the volume fraction of the second phase (air), its value ranging from 0 to 1. The volume fraction of the first phase (water) will be $1 - \alpha_2$. The rest of the symbols follow the definitions given in the nomenclature table at the end of the article. The momentum and energy equations shown in Equation-3 and 4 are shared among phases with the combined material properties. These material properties such as density ($\rho$) and dynamic viscosity ($\mu$) in the domain are calculated based on the interface location using Equation-2. Here $E$ and $T$ are the mass-weighted average energy and temperature. Similarly, the turbulent kinetic energy and dissipations are also shared among phases.

$$\rho = \alpha_2\rho_2 + (1-\alpha_2)\rho_1, \quad \mu = \alpha_2\mu_2 + (1-\alpha_2)\mu_1 \tag{2}$$

$$\frac{\partial(\rho\vec{V})}{\partial t} + \nabla.(\rho\vec{V}\vec{V}) = -\nabla p + \nabla.(\mu(\nabla\vec{V} + \nabla\vec{V}^T)) + \rho\vec{g} \tag{3}$$

$$\frac{\partial(\rho E)}{\partial t} + \nabla(\vec{V}(\rho E + p) = k_{eff}\nabla T \tag{4}$$

### 3.2 Derivation of coefficients

To understand the impact of operating conditions on the fluid's response to pressure disturbance, we begin with the 2D X-momentum equation (Equation-5) for a compressible flow with no body force, since gravity acts in the y-direction.

$$\frac{\partial u}{\partial t} + u\frac{\partial u}{\partial x} + v\frac{\partial u}{\partial y} = -\frac{1}{\rho}\frac{\partial p}{\partial x} + \nu\frac{\partial^2 u}{\partial y^2} \tag{5}$$

For simplification, only the dominating stress term is considered. Now we use reference pressure $p_{ref}$ to nondimensionalize the pressure term. Similarly, the average liquid flow speed during the steady-state is considered as the reference velocity. Finally, pipe length and diameter (height of channel in 2D) are considered reference lengths for nondimensionalizing the x and y coordinates, respectively.

$$u^* = \frac{u}{u_{ref}}, \quad v^* = \frac{v}{u_{ref}}, \quad x^* = \frac{x}{L}, \quad y^* = \frac{y}{D}$$

$$t^* = \frac{tu_{ref}}{L}, \quad p^* = \frac{p}{p_{ref}}, \quad \rho^* = \frac{\rho}{\rho_{ref}}, \quad \nu^* = \frac{\nu}{\nu_{ref}}$$

**Table 1** Design of study to analyze various combinations of coefficients

| Pipe Length (m) | $C_p$ | $C_\tau$ | Pressure Head (m) | U (m/s) |
|---|---|---|---|---|
| 1000 | 592.028 | 0.001 | 50 | 1 |
| | 59202.81 | 0.01 | 50 | 0.1 |
| | 5920281 | 0.1 | 50 | 0.01 |
| | 19962.81 | 0.01 | 10 | 0.1 |
| 100 | 592.028 | 0.0001 | 50 | 1 |
| | 59202.81 | 0.001 | 50 | 0.1 |
| | 5920281 | 0.01 | 50 | 0.01 |
| 10 | 592.02 | 1e-5 | 50 | 1 |
| | 199.628 | 1e-5 | 10 | 1 |
| | 130.95 | 3e-6 | 3 | 1 |

$$\frac{\partial u^*}{\partial t^*} + u^* \frac{\partial u^*}{\partial x^*} + \left(\frac{L}{D}\right) v^* \frac{\partial u^*}{\partial y^*} = -\left(\frac{p_{ref}}{u_{ref}^2 \rho_{ref}}\right) \frac{1}{\rho^*} \frac{\partial p^*}{\partial x^*} + \frac{\nu_{ref}}{u_{ref} D} \frac{L}{D} \nu^* \frac{\partial^2 u^*}{\partial y^{*2}} \tag{6}$$

$$\frac{\partial u^*}{\partial t^*} + u^* \frac{\partial u^*}{\partial x^*} + \left(\frac{L}{D}\right) v^* \frac{\partial u^*}{\partial y^*} = -C_p \frac{1}{\rho^*} \frac{\partial p^*}{\partial x^*} + C_\tau \nu^* \frac{\partial^2 u^*}{\partial y^{*2}} \tag{7}$$

Equation-7 highlights the key contributors to the rate of change of fluid momentum, *coefficient of pressure gradient*, $C_p$, and *coefficient of shear stress rate*, $C_\tau$ ($C_\tau = \frac{1}{Re}\frac{L}{D}$). The coefficient of pressure gradient amplifies the pressure gradient contribution, which supports the disturbance in the system and thereby the generation of slugs. In contrast, the term coefficient of shear stress rate amplifies damping effects and prevents the formation of slugs. The $L/D$ ratio on the left hand side influences response on the gradient, i.e, larger value of this ratio will result in lower convective acceleration.

Similarly, the Y-momentum equation can also be deduced and parameters like Froude number can be obtained. However, these parameters are not considered in the current study.

### 3.3 Numerical methodology

We have investigated various pressure and velocity conditions to realize good spread in the coefficients' vector. Also, three different pipe length are assessed- 1000m, 100m, and 10m, to identify the effect of pipe length on the results. The mesh refinement and boundary layers are comparable to previous works [3, 16]. In the VOF solver setup, air is treated as compressible gas assuming ideal gas behavior, whereas water is treated as an incompressible liquid. Flow and energy equations are solved with second-order accuracy, and that of turbulence equations are solved with first-order accuracy. A time step of $0.001s$ is used for forcing frequency $0.1Hz$, and $1Hz$, and $0.01s$ is used for forcing frequency $0.01Hz$. At least one period of excitation is solved

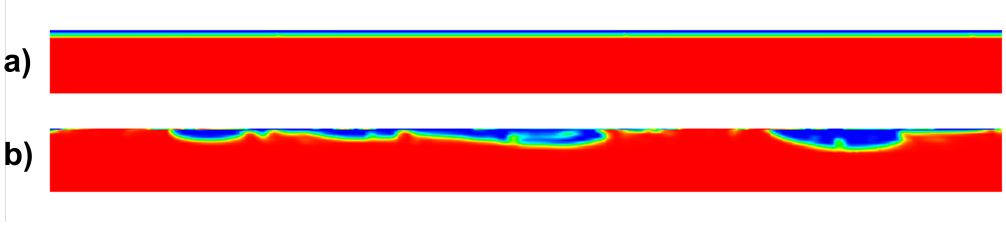


**Fig. 1** Stratified to Slugs flow with exciting frequency of 0.1 Hz for condition $C_P$ as 5920281 and $C_\tau$ as 0.01. Due to large length of the pipe, cropped image is shown here. Here image a) is showing steady stratified flow and b) is showing instantaneous image of slug

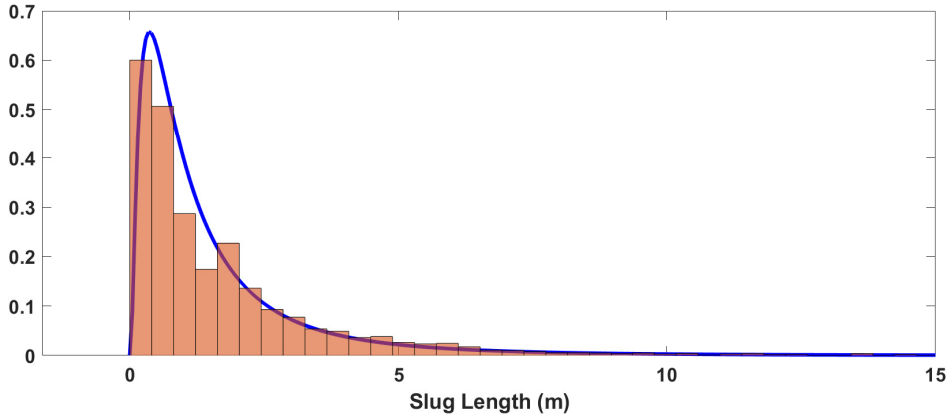


**Fig. 2** Normalized histogram and probability distribution of slug length generated in the 100 m pipe for $C_p$ 59202.81, disturbed by forcing frequency 0.1 Hz

for each case to realize saturation of slug formation. The inlet boundary is treated as total pressure boundary and that of the outlet boundary as pressure outlet. The walls are treated as no-slip and adiabatic. Also, the interface position at an inlet is fixed at 0.8 m to 0.9 m, depending on the superficial velocity. A similar interface position is applied to the backflow outlet boundary. The final steady stratified flow is shown in Fig-1 where the interace is close to wall depicting high value of $C_p$. The design of the study is summarized in Table-1. For each condition, we achieved a steady-state flow condition using pressure boundary on the inlet and outlet.

$$p_2' = p_2 \left(1 + 0.2sin(2\pi ft)\right) \tag{8}$$

The steady flow condition is now disturbed by modifying the outlet pressure boundary with harmonic excitation of amplitude 20 percent of outlet pressure with the single frequency as shown in Equation-8. The simulation is repeated with three different frequencies $0.01Hz, 0.1Hz$, and $1Hz$. The amplitude and frequency of disturbances are chosen from the study of geyser simulation, where the spectral analysis of the pressure fluctuations shows that the frequency larger than $1Hz$ is a significant contributor. Also, the amplitude of disturbance is generally 20 percent of the total head [12]. The 20 percent amplitude is used for all the simulations. However, this is also an important variable that is not considered in this study.

## 4. RESULTS AND DISCUSSION

The analysis and visualization of slug formation are carried out using the stored animation frames for each case. Vector-based image processing techniques are used to detect slugs. Fig-2 shows the normalized histogram and probability distribution of the slug's length. One can observe the shape of the distribution is log-normal, which is also shown by Nydal et al. [15]. Also, Fig-3 shows the distribution of slugs along the length for pipe of 1000 m and 100 m for the same operating condition. In the case of a long pipe, slugs are populated near the outlet boundary, whereas the shorter pipe shows the slugs distributed in the entire pipe. However, in both cases, the region of influence is around $100m$, and one can infer how the effect of disturbances fade away with distance. This behavior can be justified because the slugs are generated due to excitation of pressure gradient term, the effect of which is damped by the shear stress rate term in the Equation-7, which gets amplified with length. Also, the cross-correlation function in MATLAB [13] is used to calculate the instantaneous averaged slugs velocity in the pipe. The averaged slugs velocity shows the harmonic relationship with time, with the same order of the forcing frequency. The comparison of the interface curves with time indicates the slugs are naturally generated at various locations. Also, their rate of displacement is aggressive initially due to the high amplitude of the disturbance, but it eventually gets slower as the forcing function completes the

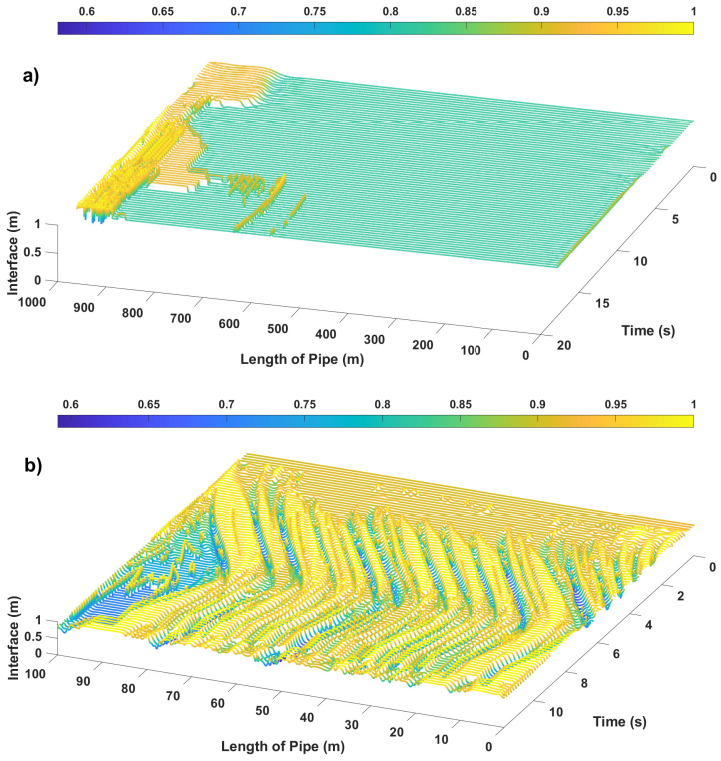


**Fig. 3** Production of slugs along the length of the pipe with time for $C_p$ 5920281 and forcing frequency $0.1Hz$. Each curve represents interface height at a given instant of time. The color bar depicts the Y-position of the interface in meters. Images a) and b) show interface curves for 1000 m and 100 m pipes, respectively.

half cycle.

Fig-4 compares the slug lengths for three different $C_p$ values negligibleat the same exciting frequency of 0.01 Hz and pipe length (100 m). We can observe that the slug length is directly proportional to $C_p$. Also, we can see that the slug is not completely composed of water, but has air entrapped within; known as aeration of slugs, this phenomena was also observed in an experimental study by Saini et al.[17]. The aeration of slugs seems uniform for all three cases; this shows $C_p$ has negligible impact on the aeration.

Next we compare the slug lengths generated in a 100 m pipe for three different exciting frequencies, keeping the value of $C_p$ constant at 59202.81. The results of this simulation case scenario are shown in Fig-5. It is seen that the slug length decreases as exciting frequency increases, which is intuitive. Also, the number of slugs formed increases with the frequency. We attribute this outcome to the fact that higher exciting frequencies reduce the impact of harmonic disturbances, and hence, we observe smaller slug formations. These are interesting findings for the storm sewer geyser research where a broad range of frequencies(0.0001 to 100 Hz) are observed at the pipe junction due to the release of trapped air, which probably transforms stratified flow in the slug flow. Slug generations are believed to be the precursor of the geyser phenomenon. Based on this result, we can attribute that the formation of slugs during the geyser is mostly due to the low-frequency disturbance (less than 0.1 Hz), and its length is directly proportional to the $C_p$.

The detail analysis of the slug's characteristics are carried out by considering all the cases mentioned in Table-1. Each case is simulated for 1 to 10 oscillation cycle and animation frames are captured at appropriate frequencies and using this frames, a time-averaged slug's characteristics are calculated. Since the exciting frequency plays a major role in the slug characteristics, the length and velocity of the slugs are normalized using characteristic velocity ($L * f$) and characteristic length ($U/f$).

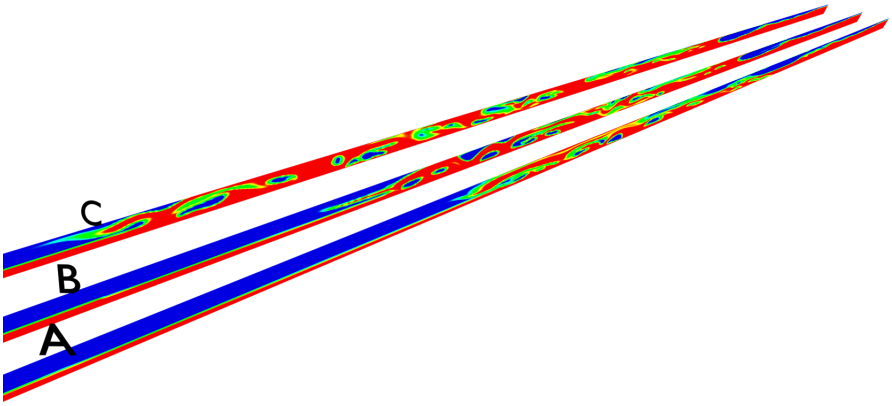


**Fig. 4** Comparison of slug length for three different $C_p$ for same excitation frequency. Labels A, B and C represents $C_p$ of 592.028, 59202.81 and 5920281 respectively.

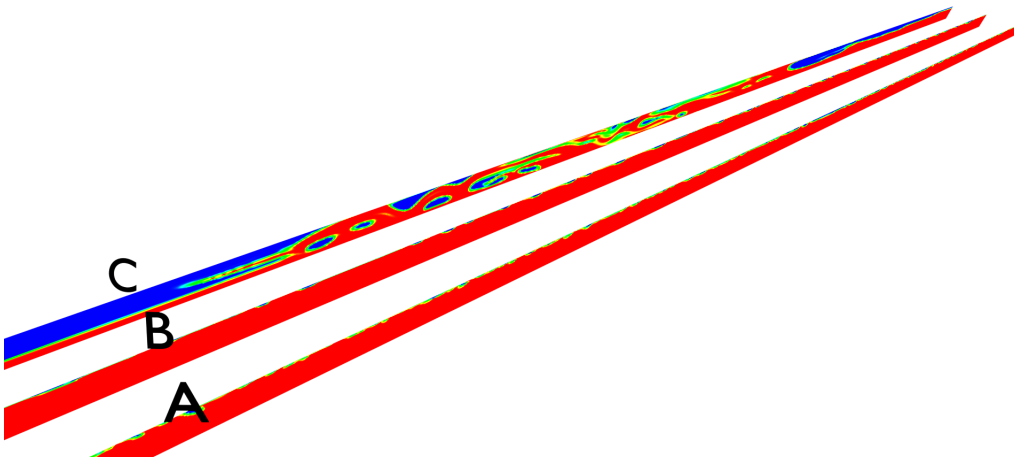


**Fig. 5** Comparison of slug length for three different frequencies for the same $C_p$. Labels A, B and C represents frequency 1, 0.1 and 0.01 Hz respectively.

### 4.1 Effect of $C_p$

The normalized slug length ($\phi$) and velocities ($\psi$) as a function of $C_p$ are shown in Fig-6 and Fig-7 for all the three frequencies. The normalized slug length varies linearly with $C_p$ on the log scale, and it is directly proportional to the forcing frequency. From the PDF analysis of the slug length for the same operating conditions, the lower frequency of excitation showed narrow distribution producing a large number of small slugs. In contrast, in the case of higher frequency, the slugs distribution is broader, showing larger slug production. For the higher value of pressure coefficient, the flow initially generates a large number of smaller slugs, but the average slug length increases significantly due to coalescence. This is evident from the histogram, which shows multiple peaks for some large slug lengths.

The normalized slug velocities seem invariant with the pressure coefficient. However, it does vary with the frequency of excitation. As expected, the lower frequency produces larger mean pressure gradients and, as a result, gives a larger slug velocity. Apart from plots and statistical results, the visual observation of the animation video (https://youtu.be/ovhbxvjGeYs) clearly shows the impact of $C_p$ and $C_\tau$ in the shape and size of the slugs. The lower values of $C_p$ showed smaller and few occasional slugs. Fig-8 compares the histogram of three case with different values of $C_p$. As the $C_p$ decreases, the histogram narrows towards the lower length of the slugs, and it reduces the mean slug length.

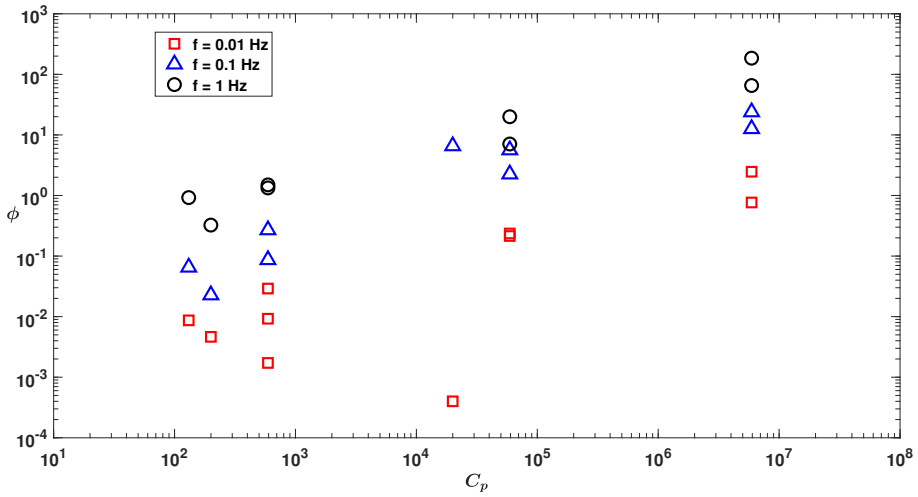


**Fig. 6** Effect of $C_p$ on the normalized slug length $\phi$ for all the three forcing frequencies.

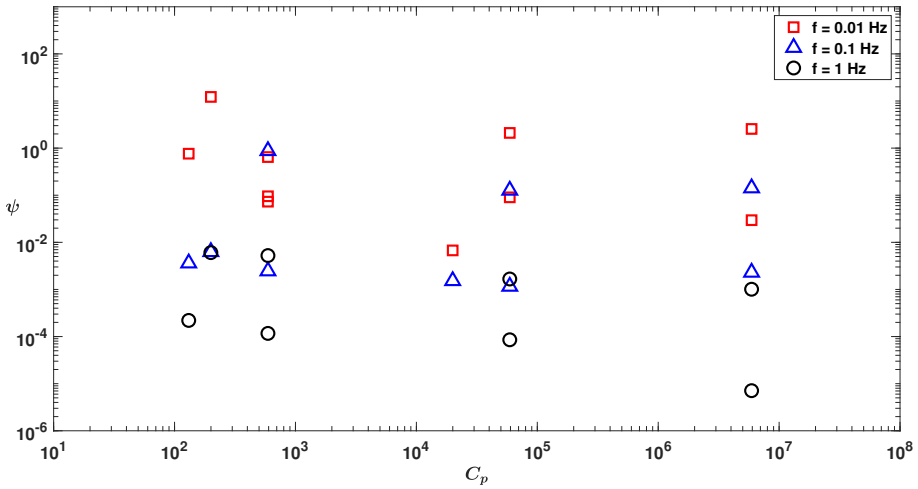


**Fig. 7** Effect of $C_p$ on the normalized slug velocity $\psi$ for all the three forcing frequencies.

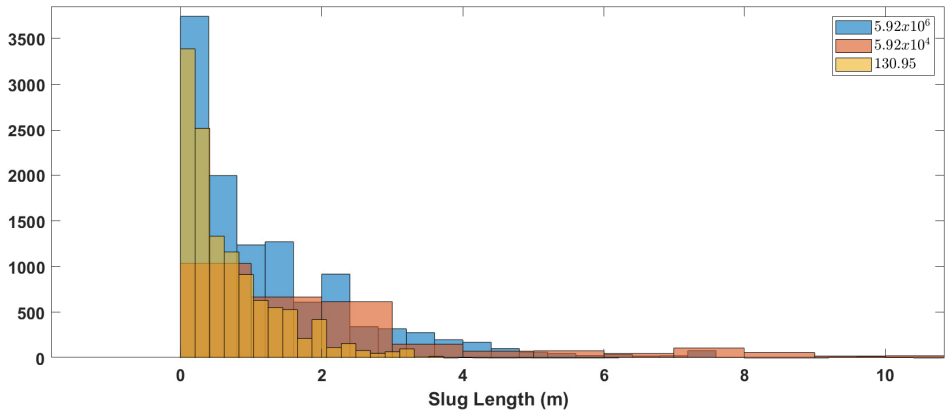


**Fig. 8** Effect of $C_p$ on actual slug length distribution for a forcing frequency of $0.1Hz$ and pipe length $100m$.

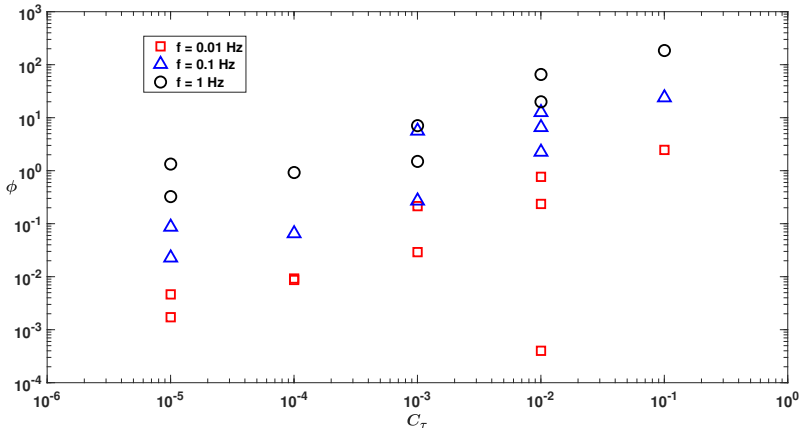


**Fig. 9** Effect of $C_\tau$ on the normalized slug length $\phi$ for all the three forcing frequency.

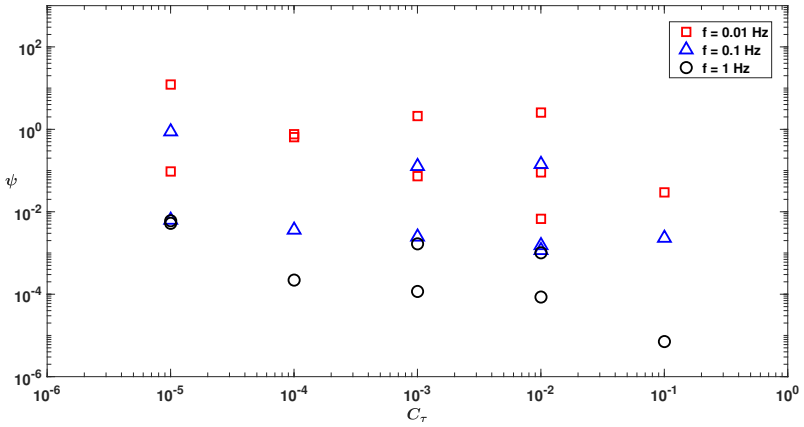


**Fig. 10** Effect of $C_\tau$ on the normalized slug velocity $\psi$ for all the three forcing frequency.

### 4.2 Effect of $C_\tau$

The effect of the shear stress rate coefficient on the normalized slug length and velocity is shown in Fig-9 and Fig-10 respectively. The plot shows the logarithmic relation of normalized slug length with $C_\tau$, which is directly proportional to the excitation frequency. As the stress coefficient increases, the effect of pressure gradient reduces, which is an adverse condition for the frequent small slugs generation. However, the damped pressure gradient allows large amplitude waves that result in large slugs. On the slug velocity side, the larger shear stress rate coefficient enhances the viscous losses and hence, reduces the slug's momentum.

## 5. CONCLUSIONS

In summary, the relation between slug formation and the operating conditions is established using the non-dimensional analysis of the X-momentum equation. The derived coefficients of pressure gradient and shear stress rate show a strong impact on the slug characteristics such as length and velocity. The coefficient of the pressure gradient is found to be strongly influencing normalized slug length, whereas the coefficient of shear stress rate has a strong negative influence on the normalized slug velocity. For lower frequency, the histogram is narrowed to lower length, whereas, for a higher frequency, it is broad and shows multiple peaks. The practical system such as oil pipes or air-conditioning pipes where stratified flow is subjected to the natural disturbance may have broad range of frequency and this methodology might help in identifying the range of

frequencies that can lead to an unwanted slug generations. Also, the derived coefficients values can help designers and operators to avoid extreme values that are prone to slug formations. As a follow-up study, we will investigate the impact of disturbance amplitude and analyze the slugs' three-dimensional features and validate this hypothesis using experimental study with PIV (Particle Image Velocimetery) measurement. Also, we would extend this work by investigating the characteristics of the slugs generated during geyser experiments and simulations for different conditions.

## ACKNOWLEDGMENTS

The authors gratefully acknowledge the financial support of the National Science Foundation (NSF) under Grant number 1928850. The views expressed are solely those of the authors. NSF does not endorse any products or commercial services mentioned.

## NOMENCLATURE

| | | |
|---|---|---|
| x | Horizontal position | (m) |
| y | Vertical position | (m) |
| u | X component of velocity | ( $m/s$ ) |
| v | Y component of velocity | ( $m/s$ ) |
| p | Static pressure | ( Pa ) |
| ρ | Density | ( $kg/m^3$ ) |
| t | Time | ( s ) |
| ν | Kinematic viscosity | ($m^2/s$) |
| μ | Dynamic viscosity | (Pa-s) |
| L | Length of the pipe | (m) |
| D | Diameter of the pipe | (m) |
| f | Forcing frequency | (Hz) |
| H | Pressure head | (m) |
| U | Superficial velocity | ( $m/s$ ) |
| $\vec{V}$ | Velocity vector | ( $m/s$ ) |
| $\alpha_2$ | Volume fraction of air | (-) |
| $\alpha_1$ | Volume fraction of water | (-) |

| | | |
|---|---|---|
| $Re$ | Reynold number | (-) |
| $C_p$ | Coefficient of pressure gradient | (-) |
| $C_\tau$ | Coefficient of shear stress rate | (-) |
| $L_{slug}$ | Slug length | (m) |
| $U_{slug}$ | Slug velocity | (m/s) |
| ϕ | Normalized slug length ($L_{slug} * f/U$) | (-) |
| ψ | Normalized slug velocity ($\frac{U_{slug}}{L*f}$) | (-) |
| $u_{ref}$ | Reference velocity | ( $m/s$ ) |
| $p_{ref}$ | Reference pressure (101325+$\rho_{ref}$gH) | ( Pa ) |
| $\rho_{ref}$ | Reference Density (998) | ( $kg/m^3$ ) |
| $t_{ref}$ | Reference time scale | ( s ) |
| $\nu_{ref}$ | Reference Kinematic viscosity | ($m^2/s$) |
| g | Gravitational acceleration | ($m/s^2$) |
| $k_{eff}$ | Effective thermal conductivity | ($W/(m.K)$) |
| T | Temperature | (K) |
| E | Total energy | (J/kg) |

## REFERENCES

[1] *Ansys® Academic Research Fluent, Release 2019 R1*.

[2] Al-Safran, E., "Investigation and prediction of slug frequency in gas/liquid horizontal pipe flow," *Journal of Petroleum Science and Engineering*, 69(1-2), pp. 143–155, (2009).

[3] Chegini, T. and Leon, A. S., "Numerical investigation of field-scale geysers in a vertical shaft," *Journal of Hydraulic Research*, 58(3), pp. 503–515, (2020).

[4] Conte, M. G., Hegde, G. A., da Silva, M. J., Sum, A. K., and Morales, R. E., "Characterization of slug initiation for horizontal air-water two-phase flow," *Experimental Thermal and Fluid Science*, 87, pp. 80–92, (2017).

[5] Davies, R. M. and Taylor, G. I., "The mechanics of large bubbles rising through extended liquids and through liquids in tubes," *Proceedings of the Royal Society of London. Series A. Mathematical and Physical Sciences*, 200(1062), pp. 375–390, (1950).

[6] Dukler, A. E. and Hubbard, M. G., "A model for gas-liquid slug flow in horizontal and near horizontal tubes," *Industrial & Engineering Chemistry Fundamentals*, 14(4), pp. 337–347, (1975).

[7] Greskovich, E. J. and Shrier, A. L., "Slug frequency in horizontal gas-liquid slug flow," *Industrial & Engineering Chemistry Process Design and Development*, 11(2), pp. 317–318, (1972).

[8] Griffith, P. and Wallis, G. B., "Two-phase slug flow," *Journal of Heat Transfer*, 83(3), (1961).

[9] Hubbard, M. and Dukler, A., "paper presented at the asme national meeting," *Tampa, Fla*, (1968).

[10] Issa, R. and Kempf, M., "Simulation of slug flow in horizontal and nearly horizontal pipes with the two-fluid model," *International journal of multiphase flow*, 29(1), pp. 69–95, (2003).

[11] Jepson, W. and Taylor, R., "Slug flow and its transitions in large-diameter horizontal pipes," *International journal of multiphase flow*, 19(3), pp. 411–420, (1993).

[12] Leon, A. S., Elayeb, I. S., and Tang, Y., "An experimental study on violent geysers in vertical pipes," *Journal of hydraulic research*, 57(3), pp. 283–294, (2019).

[13] MATLAB, *version 9.8.0.1417392 (R2020a)*, The MathWorks Inc., Natick, Massachusetts, (2020).

[14] Mishima, K. and Ishii, M., "Theoretical prediction of onset of horizontal slug flow," (1980).

[15] Nydal, O., Pintus, S., and Andreussi, P., "Statistical characterization of slug flow in horizontal pipes," *International Journal of Multiphase Flow*, 18(3), pp. 439–453, (1992).

[16] Olbrich, M., Schmeyer, E., Bär, M., Sieber, M., Oberleithner, K., and Schmelter, S., "Identification of coherent structures in horizontal slug flow," *Flow Measurement and Instrumentation*, 76, pp. 101814, (2020).

[17] Saini, S. and Banerjee, J., "Physics of aeration in slug: Flow visualization analysis in horizontal pipes," *Journal of Visualization*, pp. 1–14, (2021).

[18] Taitel, Y. and Dukler, A., "Effect of pipe length on the transition boundaries for high-viscosity liquids," *International journal of multiphase flow*, 13(4), pp. 577–581, (1987).